Neuroscience 310 (2015) 600–615

TASK-SPECIFIC STABILITY OF ABUNDANT SYSTEMS: STRUCTURE OF VARIANCE AND MOTOR EQUIVALENCE

D. MATTOS, [a,b,d]* **G. SCHÖNER,** [c] **V. M. ZATSIORSKY** [d] **AND M. L. LATASH** [d]

[a] *Biomechanics and Movement Science Program, University of Delaware, Newark, DE, United States*

[b] *Program in Occupational Therapy, Washington University, Saint Louis, MO, United States*

[c] *Institut für Neuroinformatik, Rühr University Bochum, Bochum, Germany*

[d] *Department of Kinesiology, The Pennsylvania State University, University Park, PA, United States*

Abstract—Our main goal was to test a hypothesis that transient changes in performance of a steady-state task would result in motor equivalence. We also estimated effects of visual feedback on the amount of reorganization of motor elements. Healthy subjects performed two variations of a four-finger pressing task requiring accurate production of total pressing force (F_{TOT}) and total moment of force (M_{TOT}). In the Jumping-Target task, a sequence of target jumps required transient changes in either F_{TOT} or M_{TOT}. In the Step-Perturbation task, the index finger was lifted by 1 cm for 0.5 s leading to a change in both F_{TOT} and M_{TOT}. Visual feedback could have been frozen for one of these two variables in both tasks. Deviations in the space of finger modes (hypothetical commands to individual fingers) were quantified in directions of unchanged F_{TOT} and M_{TOT} (motor equivalent – ME) and in directions that changed F_{TOT} and M_{TOT} (non-motor equivalence – nME). Both the ME and nME components increased when the performance changed. After transient target jumps leading to the same combination of F_{TOT} and M_{TOT}, the changes in finger modes had a large residual ME component with only a very small nME component. Without visual feedback, an increase in the nME component was observed without consistent changes in the ME component. Results from the Step-Perturbation task were qualitatively similar. These findings suggest that both external perturbations and purposeful changes in performance trigger a reorganization of elements of an abundant system, leading to large ME change. These results are consistent with the principle of motor abundance corroborating the idea that a family of solutions is facilitated to stabilize values of important performance variables. Published by Elsevier Ltd. on behalf of IBRO.

Key words: motor equivalence, synergy, finger force, perturbation, uncontrolled manifold hypothesis.

INTRODUCTION

All natural human movements involve more elements than necessary to perform typical tasks and, hence, allow numerous ways of performing such tasks. In each particular case, a single solution is observed from a potentially infinite set. How do such single solutions emerge? This question constitutes the essence of the so-called problem of motor redundancy, or the Bernstein problem (Bernstein, 1967; Turvey, 1990). Earlier approaches assumed that the central nervous system (CNS) added constraints (eliminated redundant degrees-of-freedoms, DOFs) and/or used optimization principles to find unique solutions each time a movement is produced (Vereijken et al., 1992; Prilutsky and Zatsiorsky, 2002).

More recently, two theoretical advances have led to different approaches to the problem of motor redundancy. The first is the principle of abundance (Gelfand and Latash, 1998; Latash, 2012). According to these ideas, the CNS does not select unique solutions to motor problems but unites all the elemental variables of apparently redundant sets in a way that facilitates families of solutions equally able to solve the task within a permissible error margin.

The second is the idea of task-specific stability (Schoner, 1995) formalized within the uncontrolled manifold (UCM) hypothesis (Scholz and Schoner, 1999). We view stability as the ability of a time-varying system to achieve a movement trajectory or state in cases of small, transient external perturbations. If a person performs a series of trials, each trial starts from a somewhat different initial condition. Trajectories are expected to show relatively large deviations in directions of low stability (leading to no changes in salient performance variables, along the UCM) as compared to deviations in directions of high stability (leading to changes in those variables, orthogonal to the UCM). As a result, an analysis of across-trial variance within the two sub-spaces, V_{UCM} and V_{ORT}, provides indices that serve as proxies of stability. Also, a quick change of the input, whether from the periphery

*Correspondence to: D. Mattos, Program in Occupational Therapy, Washington University School of Medicine, Campus Box 8535, 4444 Forest Park Avenue, Saint Louis, MO 63108-2292, United States. Tel: +1-314-286-1994.
E-mail address: mattosd@wusm.wustl.edu (D. Mattos).

Abbreviations: CNS, central nervous system; DOFs, degrees-of-freedoms; FTOT, total pressing force; ME, motor equivalent; MTOT, total moment of force; MVC, maximal voluntary contraction; nME, non-motor equivalent; RC, referent configuration; UCM, uncontrolled manifold.

http://dx.doi.org/10.1016/j.neuroscience.2015.09.071
0306-4522/Published by Elsevier Ltd. on behalf of IBRO.

(perturbation) or from hierarchically higher levels (action) is expected to lead to large deviations along the UCM (motor equivalent – ME).

In a series of recent studies, quick reactions to external perturbations were used to explore actions by apparently redundant (we are going to address them as "abundant") sets of elemental variables during multi-joint and multi-finger tasks (Scholz et al., 2007; Mattos et al., 2011, 2013, 2015). These studies have shown that correction of a perturbation leads to a large amount of ME motion in the space of elemental variables. Commonly, ME deviations were much larger than those leading to changes in the perturbed performance variable (non-motor equivalent – nME). Such large amounts of the apparently wasteful ME deviation were interpreted to reflect low stability within the corresponding UCM. This interpretation is complicated by a few factors. First, in some of the mentioned studies (Mattos et al., 2011, 2013), the perturbation acted during the entire movement time and, hence, in perturbed trials, the task was performed in a different force field. Second, even in studies with transient perturbations (Mattos et al., 2015), effects of the perturbations could last for some time and superimpose on the effects of the corrective actions. One of the main goals of the current study has been to address these problems and explore the amounts of ME and nME change when task demands are modified rapidly and transiently. Our primary hypothesis was that the relationship between ME and nME components would be task-specific.

We also explored the role of sensory signals of different modalities in bringing about the large amounts of ME motion during corrective actions. Note that in earlier studies the subjects received both visual and natural somatosensory feedback. In this study, we turned visual feedback off for one of the two performance variables, total pressing force (F_{TOT}) or total moment of force (M_{TOT}). Our secondary hypothesis was that the amount of ME motion would be insensitive to the presence of visual feedback, while nME motion would increase without visual feedback. This hypothesis is based on the idea of back-coupling feedback loops from motion-sensitive somatosensory receptors to neural mechanisms ensuring task-specific stability (Latash et al., 2005; Martin et al., 2009). These circuits are expected to function in the absence of visual feedback leading to high ME motion, while drifts in the performance variables are expected (Vaillancourt and Russell, 2002; Ambike et al., 2015) resulting in larger nME motion.

To address these hypotheses, we used two tasks. Both tasks required the subjects to produce accurate combinations of F_{TOT} and M_{TOT} by a set of four fingers. In task 1, no perturbation was applied while the target could jump requiring a quick change in F_{TOT} or M_{TOT}; after a short delay, the target jumped to the initial state. Visual feedback was provided for the "jumped" variable, while it was frozen for the other variable. In the second task, a finger was perturbed (lifted) using the "inverse piano" device (Martin et al., 2011). This led to changes in both F_{TOT} and M_{TOT}. Visual feedback was available at all times for one of these variables and frozen for the other variable.

EXPERIMENTAL PROCEDURES

Subjects

Eight healthy young adult subjects (mean age 30.37 ± 5.10 years; six male, two female) took part in this study. All subjects were self-reported right-hand dominant and had no history of injury or pain in the upper limb for the last six months. Subjects signed the informed consent form as approved by the Office for Research Protection of the Pennsylvania State University.

Equipment

The "inverse piano" device (Fig. 1, right panel) was used to provide finger perturbations (Martin et al., 2011). This equipment consists of four unidirectional piezoelectric force sensors (208C01; PBC Piezotronics Inc.; Depew, NY, United States) mounted within slots of a steel frame (140 × 90 mm), 3-cm apart in the mediolateral direction. The anterior-posterior position of the sensors was adjusted to fit the individual subject's anatomy. Each sensor was covered with sandpaper (300 grit) and connected to linear actuators (PS01-23x80; LinMot). The signals coming from the sensors were sent through a DC-coupled signal conditioner (PCB) to a 16-bit analog-to-digital converter (CA-1000; National Instruments). A customized Labview program (National Instruments) was written to acquire and record the individual force signals at 200 Hz, and also to control the linear actuators through a controller (E-400-AT; LinMot). The timing of perturbation onset was recorded.

Procedure

Subject position. Subjects sat on a chair with their right arm resting on a table. In the initial position, the upper arm was slightly abducted, 60° of shoulder abduction, 120° of elbow flexion, forearm pronated, and the wrist in neutral position. Cushioned paddings were placed under the forearm and hand for comfort. The forearm was secured to the platform with two straps to stabilize the initial posture. A monitor was placed 0.8 m away from the subject, at the eye level. The monitor was used to set tasks and provide visual feedback. The subject position is illustrated in Fig. 1.

Experimental task. This study consisted of two main experiments preceded by maximal voluntary contraction (MVC) finger pressing tasks and one-finger tasks with accurate ramp force production (Ramp-tasks). In every trial, the subjects started with all four fingers (I: index, M: middle, R: ring and L: little) relaxed on the top of the force sensors facing the computer display. Then, the sensor signals were set to zero, which allows recording voluntary downward forces without an effect of fingers/hand's weight. Once the subject was ready, data collection started.

MVC task. Subjects were instructed to press as hard as possible on the sensors with all four fingers for 6 s. Visual feedback on the total force profile was provided

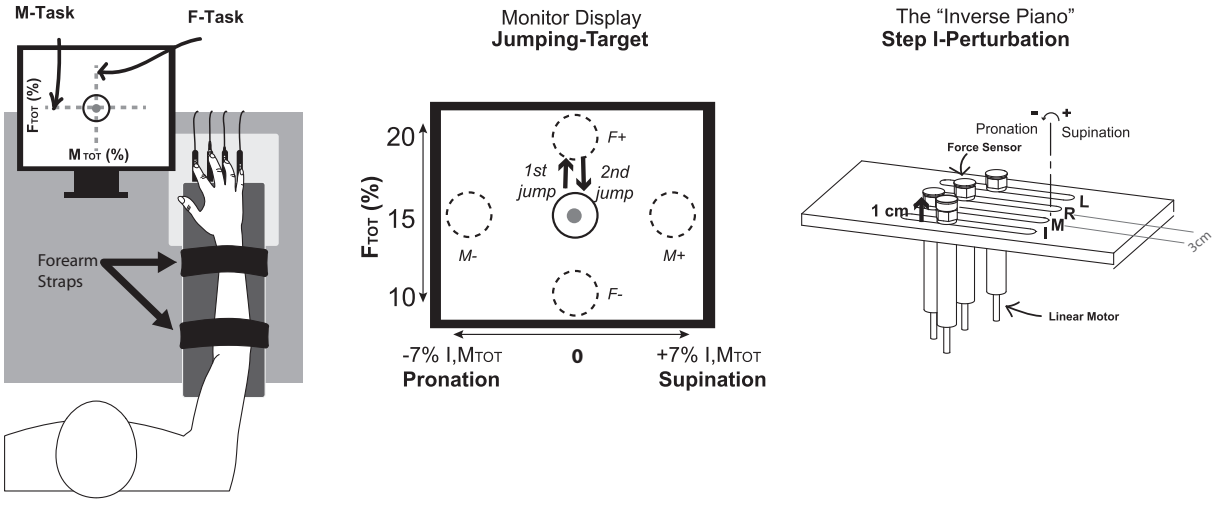

Fig. 1. *Left:* The experimental setup. The monitor shows the target position at the beginning of each trial and the cursor feedback for the F- and M-tasks. *Middle:* Visual feedback for the Jumping-Target task with the four possible conditions of target jump. Only one target was shown at each time. *Right:* The inverse piano used to lift the index (I) finger during the Step I-Perturbation task. The zero moment was computed with respect to the midline between middle (M) and ring (R) fingers. Clockwise direction was considered (+) and represented supination moment of the forearm.

as well as verbal encouragement. The maximal peak total force between two attempts was chosen as MVC. The MVC task was used to normalize the force and moments of force used in the main experimental tasks.

Ramp-task. Subjects placed the four fingers on the sensors and tracked a ramp template displayed on the monitor with one finger at a time. The ramp had three segments, two horizontal lines at 0% and 8% of MVC for 4 s, with an oblique line in-between from 0% to 8% MVC over 6 s. After a couple of practice trials, two trials were collected for each finger, and the trial with the trace most closely following the template was used to compute finger modes (see below). This task was used to estimate unintended finger force production by non-instructed fingers as reflected in the enslaving matrix (Zatsiorsky et al., 1998). We used the enslaving matrix to convert finger forces into finger modes, hypothetical central command to fingers that can be manipulated by the CNS one at a time, at least hypothetically. Modes reflect combinations of commands to all four fingers of a hand (such as their referent coordinates, Pilon et al., 2007) when a person tries to press with a specific finger.

Main tasks (Jumping-Target and I-Perturbation tasks). Subjects performed several target-matching tasks. The visual target consisted of a white circle, 1.5-cm in diameter, placed at the center of the screen. A moving cursor (a dot with the diameter of 1 mm) was shown online, with the *x*-coordinate corresponding to M_{TOT}, and *y*-coordinate corresponding to F_{TOT} as illustrated in Fig. 1 (left panel). Zero value of M_{TOT} relative to the midline between the M and R fingers corresponded to the center of the screen and zero F_{TOT} corresponded to the bottom of the screen.

At the trial onset, the target was always located at the center of the screen corresponding to F_{TOT} = 15% MVC and zero M_{TOT}. Individuals were instructed to bring the cursor into the center of the target as quickly and accurately as possible, and to keep the cursor inside of the target until the end of the trial. Pilot trials showed that individuals usually take ≈ 2 s to bring the cursor into the target, and to stabilize the required combination of F_{TOT} and M_{TOT}. For all trials, further manipulations, such as target "jumps" on the screen or perturbation of the I-finger (see later) started randomly between 5 and 7 s from the start of the trial. Each trial lasted 15 s.

Jumping-Target task. This part of the experiment (Fig. 1, middle plots) involved quick changes in the target position. In those trials, the target suddenly assumed a new position on the screen, remained in that position for 4 s, and then returned to its initial position (F_{TOT} = 15% MVC and M_{TOT} = 0) until the end of the trial. The subjects were instructed to always keep the cursor in the middle of the target, which required quick changes in either F_{TOT} or M_{TOT}. In the F-Jumping-Variable the target changed to either 20% (F+) or 10% (F−) of MVC. After the target jump was initiated, the *x*-coordinate of the cursor was "frozen" and supplied no information on M_{TOT}; as a result the subjects received feedback only on F_{TOT}. Similarly, in the M-Jumping-Variable, the target jumped to the right (M+, requiring supination M_{TOT}), or to the left (M−, requiring pronation M_{TOT}). The target jump amplitude corresponded to ±7% of the maximal moment produced by the I-finger. In this condition, the position of the cursor along the *y*-axis was frozen. The F- and M-Jumping-Variable trials were performed in two blocks, and the order was balanced across subjects. Each block included a total of 30 trials, with 15 trials for each direction of target jump (either F+/F− or M+/M−). Three familiarization trials for each condition were provided at the beginning of each block. There was at least a 30-s interval between the trials and breaks of 3 min before each block.

I-Perturbation task. This part of the experiment (Fig. 1, right panel) was designed to analyze differences in the inter-trial structure of variance and motor equivalence as

a function of perturbations applied to the I-finger and visual feedback. The individuals were instructed to keep the cursor in the middle of the target. At random times between 5 and 7 s from the beginning of the trial, the I-finger was smoothly lifted by 1 cm over 0.5 s. The I-finger remained lifted until the end of the trial (Step, I-Perturbation). The perturbation led to an increase in both F_{TOT} and the pronation moment. The subjects were instructed to correct the effects of the I-finger perturbation as quickly as possible and keep the cursor in the center of the target at all times. After the perturbation onset, the cursor visual feedback was manipulated in two subtasks: F- and M-Tasks. In the F-Task, only force feedback was displayed, while the cursor *x*-coordinate was frozen. In the M-Task, the moment feedback was displayed, and the *y*-coordinate was frozen. The order of F- and M-Tasks was block randomized among subjects. There were three practice trials for familiarization with the protocol at the beginning of each condition. More trials were provided as needed to guarantee that the subjects understood the task. A total of 12 trials were performed with at least 30-s intervals between them.

Procedure

The experimental tasks required simultaneous accurate production of F_{TOT} and M_{TOT}; therefore the motor equivalence and the inter-trial variance analysis in mode-forces (see computation bellow) were analyzed to test the preservation of both F_{TOT} and M_{TOT}.

Initial data processing. The acquired signals were converted into force units, and low-pass filtered at 5 Hz with the 4th-order zero-lag Butterworth filter. We used a relatively low cutoff frequency due to the vibrations seen in the signal during the finger perturbation when the actuators were active. Note, that most analyses were performed using steady-state phases. The total force was computed by summing the individual finger forces.

Enslaving matrix and finger modes. The amount of enslaving was computed using the finger forces in the oblique part of the Ramp-task. Linear regressions were performed between the individual finger forces and the total force for each instructed finger, i = (I, M, R, L), the regression coefficients (k) were used to estimate the 4×4 enslaving matrix, [E]:

$$[E] = \begin{bmatrix} k_{II} & k_{IM} & k_{IR} & k_{IL} \\ k_{MI} & k_{MM} & k_{MR} & k_{ML} \\ k_{RI} & k_{RM} & k_{RR} & k_{RL} \\ k_{LI} & k_{LM} & k_{LR} & k_{LL} \end{bmatrix} \quad (1)$$

The finger-force was converted into modes using enslaving matrix as follows:

$$\boldsymbol{m} = \boldsymbol{E}^{-1}\boldsymbol{f}, \quad (2)$$

where, $\boldsymbol{f}$ is the 4×1 finger forces vector, and $\boldsymbol{m}$ is the 4×1 finger mode vector. Further analysis was performed in the mode space, hypothetical neural commands that can be manipulated one at a time (Danion et al., 2003). We used the linear regression analysis to compute the enslaving matrix because they require only a handful of trials. Other methods, such as neural network or principal component analysis, could potentially lead to more reliable estimates (cf. Danion et al., 2003) but they would require numerous trials that could make the subjects tired and unable to perform the main part of the experiment. The relative contribution to the F_{TOT} produced by the master-fingers is represented by the diagonal entries of the $\boldsymbol{E}$ matrix, while the off-diagonal entries represent the slave-finger force contributions.

M_{TOT}. The M_{TOT} was computed with respect to a horizontal axis parallel to the forearm/hand and passing through the mid-point between the centers of the force sensors for the M and R fingers:

$$M_{TOT} = d_I f_I + d_M f_M + d_R f_R + d_L f_L, \quad (3)$$

where d_i and f_i represent the force and the lever arm for each finger i, respectively i = [I, M, R, L]. The center of the force sensors were 3-cm apart; hence, $d_I = -4.5$ cm, $d_M = -1.5$ cm, $d_R = 1.5$ cm and $d_L = 4.5$ cm. Supination and pronation moments are represented by positive and negative values, respectively. The moment estimation assumed no change in the point of application of the force in the mediolateral direction. Note that this value was not equal to the actual total pronation-supination moment.

Analysis of motor equivalence. This analysis quantified the amount of deviations in the space of finger-modes that led to either preservation of a selected performance variable, F_{TOT} or M_{TOT}, (ME component) or deviations in that variable (nME component). We quantified such deviations caused by corrective actions in both the Jumping-Target task and the I-Perturbation task. The signals were aligned by the onset of the target motion (Jumping-Target) or I-finger perturbation (I-Perturbation). For each trial, j, the average finger-mode ($m_{j,\ AV}$) produced between 2.0 and 2.5 s before the onset time was computed. In this time window the finger-modes were relatively steady. Then, the deviation vector ($\Delta m_j = m_j - m_{j,\ AV}$) between the mode ($m_j$) and the time-averaged finger-mode ($m_{j,\ AV}$) was obtained for each time sample. The mean across trials, Δm, was computed next. The Jacobian ($\boldsymbol{J}$) matrices reflect how changes in individual finger modes produce changes in F_{TOT} and M_{TOT}: $\boldsymbol{J_F} = [1, 1, 1, 1] \cdot [\boldsymbol{E}]$ and $\boldsymbol{J_M} = [d_I, d_M, d_R, d_L] \cdot [\boldsymbol{E}]$, respectively and $d_I = -4.5$ cm, $d_M = -1.5$ cm, $d_R = 1.5$ cm, and $d_L = 1.5$ cm, where the operator "·" indicates matrix multiplication. The UCM was defined as the three-dimensional null-space of the Jacobian matrix $\boldsymbol{J}$ (standing for either $\boldsymbol{J_F}$ either $\boldsymbol{J_M}$), spanned by the basis vectors $\boldsymbol{\varepsilon_i}$, ($i$ = 1, 2, 3) solving:

$$\boldsymbol{J} \cdot \boldsymbol{\varepsilon_i} = 0 \quad (4)$$

Then, mean deviation mode vector, Δm, was projected onto the null- and orthogonal spaces of the corresponding $\boldsymbol{J}$ as follows:

$$\Delta m_{\|} = \sum_{i=1}^{3} (\varepsilon_i^T \cdot \Delta m) \cdot \varepsilon_i \quad (5)$$

$$\Delta m_{\perp} = \Delta m - \Delta m_{\parallel} \quad (6)$$

where $\Delta m_{\parallel}$ is the null-space component and $\Delta m_{\perp}$, is the orthogonal component of the mean deviation mode vector. Both components are still four-dimensional mode vectors. The extent of ME and nME changes of the modes was assessed by computing the length of these vectors, normalized by the square root of the number of DOF in the corresponding dimension (DOF_{UCM} = 3, DOF_{ORT} = 1; see Mattos et al., 2011): $ME = \sqrt{\sum_{n=1}^{4} \Delta m_{\parallel,n}^2/3}$ and $nME = \sqrt{\sum_{n=1}^{4} \Delta m_{\perp,n}^2/1}$.

UCM-based variance analysis. To link the current experiment to earlier studies of four-finger force/moment production (Latash et al., 2001; Scholz et al., 2002), we also explored the structure of inter-trial variance in the space of commands to fingers (finger modes, Latash et al., 2001; Danion et al., 2003). This analysis investigated whether the trial-to-trial variance in the finger-mode combinations was compatible with changed (V_{ORT}) or consistent (V_{UCM}) value of a performance variable, F_{TOT} and M_{TOT}. For the variance analysis, at each time sample, the mean, across trials, *j*, of the mode vector, was computed and used to make the mode vector at each time sample and each trial, *j*, mean-free: the mean-free mode vector was projected onto the null (V_{UCM}) and orthogonal (V_{ORT}) spaces of the corresponding ***J*** using the basis vectors, ε_i, of Eq. (4):

$$\delta m_{\parallel j} = \sum_{i=1}^{3} (\varepsilon_i^T \cdot \delta m_j) \cdot \varepsilon_i \quad (7)$$

$$\delta m_{\perp j} = \delta m_j - \delta m_{\parallel j} \quad (8)$$

The variance across trials per DOF along (V_{ucm}) and orthogonal (V_{ort}) to the UCM was then computed as follows:

$$V_{ucm} = \sum_{j=1}^{N_{trials}} |\delta m_{\parallel j}|^2/3 \quad (9)$$

$$V_{ort} = \sum_{j=1}^{N_{trials}} |\delta m_{\perp j}|^2/1 \quad (10)$$

where the vertical bars indicate the computation of the length of each mode vector. The normalization again takes into account the dimensionality of each subspace (DOF_{UCM} = 3; DOF_{ORT} = 1).

Definition of phases of analysis. We computed the mean components of variance and ME indices within steady-state phases as illustrated in Fig. 2. For the *Jumping-Target* task, the steady-state phase "PRE-" was computed as the average value between 2.0 and 2.5 s prior to the first target jump (1st jump), the phase during target jump (DUR-) corresponded to the time window 3.0–3.5 s after the 1st jump, and the phase post-target jump was computed between 2 and 2.5 s after the second target jump, when the target returned to its initial position. For the *I-Perturbation* trials, the pre- and post-perturbation phases were computed over 2–2.5 s before and after the onset of the I-finger lifting, respectively. Note that in the PRE-phase the deviations in finger modes were computed with respect to the same time interval (see above – Analysis of motor equivalence). Thus the difference vector of the time profile of finger-mode (Δm_j) from its average ($m_{j,\ AV}$) was zero on average. The fluctuations around that mean, had ME and nME components, illustrated in the time profiles in Fig. 4 between −2.5 and −2.0 s. Because lengths were positive numbers, the mean length of either component was larger than zero.

Statistical analysis

In the Jumping-Target experiment, the Jumping-Variable could involve transient changes of either F_{TOT} or M_{TOT}. We quantified the {ME; nME} and {V_{UCM}; V_{ORT}} components with respect to both F_{TOT} and M_{TOT}. This was done to verify the effects of the quick changes in each of the variables at phases DUR- and POST-target jumps on the components. We also estimated how visual feedback removal after the target jumps affected the outcome variables. Thus, separate 3-way ANOVAs were performed to test the stability of each of the two performance variables for each Jumping-Variable. We divided the analyses of the continuous- and frozen-feedback variables. In the first one, when the target jumped to different values of force or moment, the performance variables analyzed were F_{TOT} and M_{TOT}, respectively. In the second case, the performance variable was M_{TOT} when force changed, and F_{TOT} when moment changed. The factors of the 3-way ANOVAs were: *Projection Component* (ME vs. nME or V_{UCM} vs. V_{ORT}), *Phase* (PRE-, DUR-, and POST-) and *Direction*. *Direction* had two levels, F+ and F− for the F-Jumping-Variable, and M+ and M− for the M-Jumping-Variable.

In the I-Perturbation experiment, we also provided visual feedback only on force (F-task) or only on moment (M-task). Note that in this experimental design the external perturbation was always the same for both conditions of visual feedback. To test the effects of perturbation and visual feedback we performed 3-way ANOVAs for the F_{TOT} and M_{TOT} separately. The factors were: *Projection Component* (ME vs. nME or V_{UCM} vs. V_{ORT}), *Phase* (PRE- and POST-), and *Task* (F- and M-Task).

The Greenhouse-Geisser adjustment to the DOFs was applied whenever violations of sphericity were observed. Two-way ANOVAS and paired *t-tests* were performed for target post hoc comparisons. Bonferroni corrections were applied. *Paired t-tests* were also performed to compare differences in the finger forces and moment of force between PRE- and POST-phases. The level of significance was set to 0.05. All statistics were performed with SPSS statistical software (v. 20, IBM).

RESULTS

Jumping-Target tasks

In this part of the experiment, the target jumps could lead to a change in the target location along the vertical axis

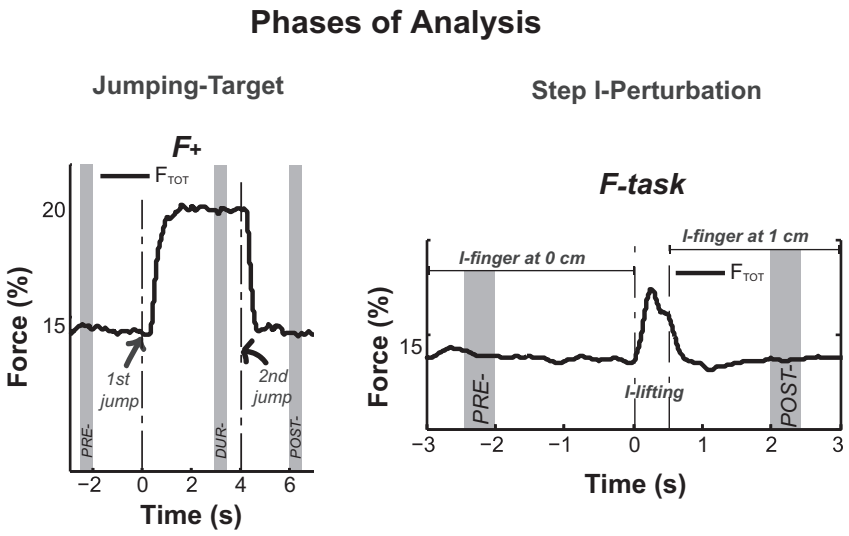

Fig. 2. Phases of analysis for the Jumping-Target and Step I-Perturbation tasks. For the Jumping-Target task, the phase PRE-corresponded to the mean values between 2.0 and 2.5 s prior to the first target jump (1st jump). The phase DUR- was computed between 3.5 and 4 s after the 1st jump. The POST-phase was computed between 2.0 and 2.5 s after the second target jump (2nd jump). For Step I-Perturbation, the phases PRE- and POST-were computed between 2.0 and 2.5 s prior to and after the onset of the index finger lifting (I-lifting), respectively.

(requiring changes in F_{TOT}) or along the horizontal axis (requiring M_{TOT} changes). Visual feedback was provided only on the Jumping-Variable, i.e. if the target jumped along the vertical axis, individuals could observe changes in F_{TOT}, while M_{TOT} visual feedback was frozen. Fig. 3 (*upper plots*) illustrates the time profiles of F_{TOT} and M_{TOT} for each of the four conditions.

As expected, the subjects kept the values of the Jumping-Variable practically unchanged after the target returned to its initial location. For F_{TOT}, the group mean ± SD was 11.05 ± 3.30 N PRE- and 11.12 ± 3.19 N ($t_7 = -1.23$, $p > 0.25$) after the target jumped up and then back to the original position (F+ Jumping-Variable); and it was 11.00 ± 3.34 N and 10.98 ± 3.19 N ($t_7 = 0.41$, $p > 0.69$), before and after the target jumped down and then back to the original position (F− Jumping-Variable), respectively. For M_{TOT}, the group mean ± SD prior and after-the target jumped to the right and then back to the original position was −0.02 ± 0.24 Nm and 0.05 ± 0.41 Nm ($t_7 = -0.39$, $p > 0.70$), respectively; and before and after the target moved to the left and then back to the original position M_{TOT} was −0.06 ± 0.26 Nm and −0.25 ± 0.46 Nm ($t_7 = 0.86$, $p > 0.41$), respectively.

In contrast, the values of the frozen-feedback variables (*i.e.* F_{TOT} for M+ and M− Jumping-Variable, and M_{TOT} for F+ and F− Jumping-Variable) showed major drifts. M_{TOT} drifted toward negative values (pronation). The group mean ± SD of M_{TOT} PRE- and POST-changes in the F+ Jumping-Variable was −0.48 ± 0.42 Nm and −6.20 ± 1.65 Nm ($t_7 = 10.59$, $p < 0.001$), respectively; and PRE- and POST-changes in the F− Jumping-Variable, M_{TOT} was −0.27 ± 0.20 Nm and −5.83 ± 2.10 Nm ($t_7 = 7.82$, $p < 0.001$), respectively. The drifts in F_{TOT} were not consistent across subjects; the standard deviations were large (∼5 N). Therefore, although F_{TOT} showed large deviations from the initial value in the M-tasks, there were no significant differences between F_{TOT} PRE- and POST-target jumps (all $t_7 < 1.845$, $p > 0.1$).

The respective changes in the individual finger forces and moments for the Jumping-Variable with continuous and frozen-feedback during the course of the trial can be seen in the middle and lower panels of Fig. 3. For the continuous-feedback variable, there were large changes in the relative amount of force produced by the M and L-fingers when the target returned to the initial position across conditions (all $|t_7| > 2.63$, $p < 0.05$), the I- and R-fingers showed less consistent changes across subjects. There were also changes in the moment of force magnitudes, but with large variability among subjects.

Motor equivalence analysis. Fig. 4 presents the ME and nME components for a representative subject, i.e., the amount of deviations in the mode space that left the performance variable unchanged, or changed, respectively. The area highlighted in gray shows the 4-s time window between the two target jumps, to a new location and back to the old location on the screen.

The analysis of the continuous-feedback variable is shown in the upper plots of Fig. 5. The ME and nME components were compared PRE- and POST-the sequence of two jumps, i.e., when the target was in the same place on the screen. For the F_{TOT} continuous-feedback variable, the ANOVA showed a significant 3-way interaction *Projection Component* × *Phase* × *Direction* on F_{TOT} ($F_{1.370,9.592} = 12.20$; $p < 0.005$), and a significant 2-way interaction *Projection Component* × *Phase* ($F_{1.483,10.384} = 12.20$; $p < 0.001$) for M_{TOT}. Prior to the first target jump, the ME (solid lines) component was significantly larger than nME (dotted lines) in F_{TOT} ($p < 0.05$). This effect was likely related to the variance structure and is discussed in detail in the Discussion. No differences between components were observed in M_{TOT} at PRE-phase

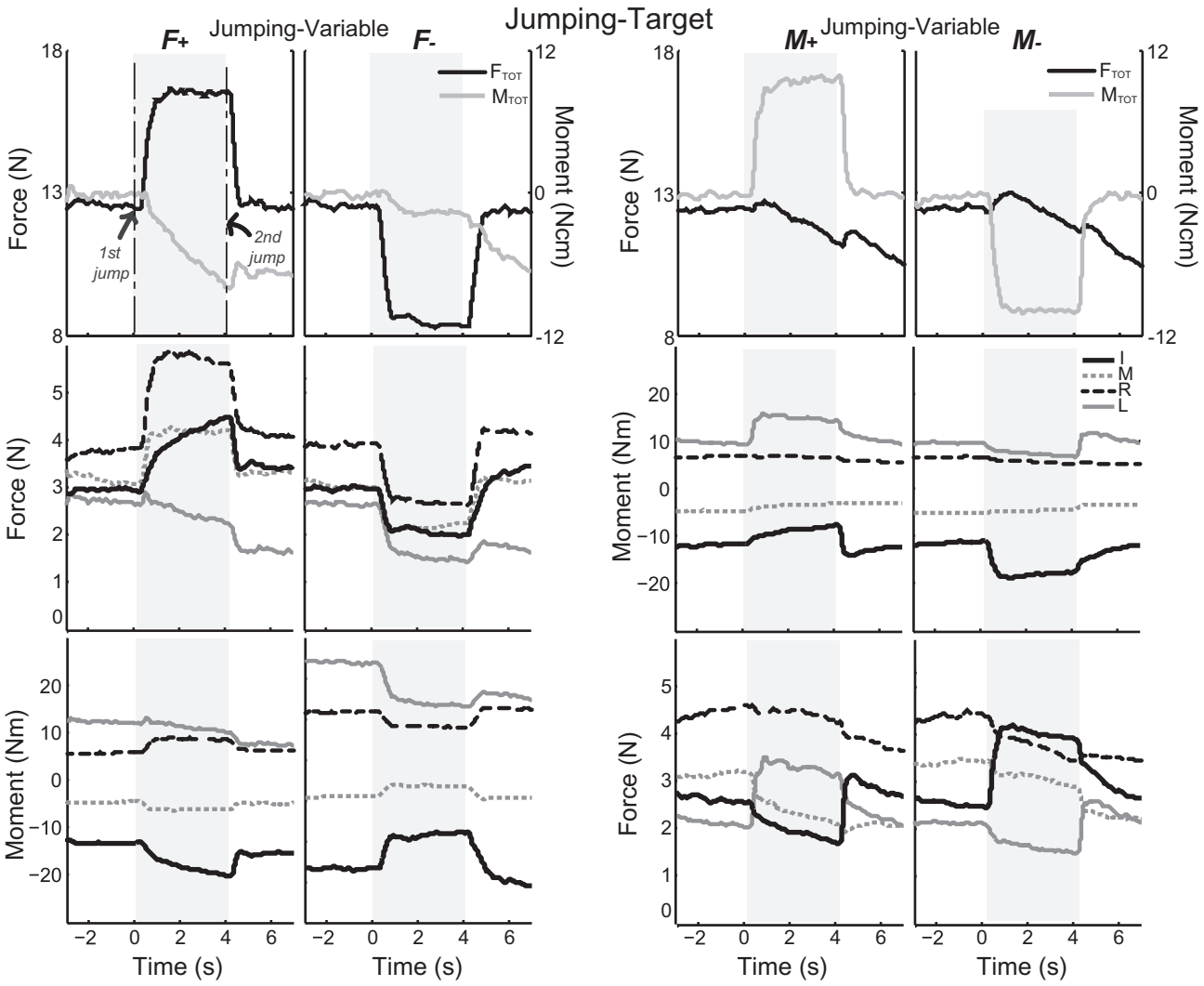

Fig. 3. Force and moment time profiles of a subject during the Jumping-Target task. The period highlighted in gray shows the target at a new position after the 1st jump. *Upper* plots show the total force (F_{TOT}) and the total moment of force (M_{TOT}) during each condition of target jump. *Middle* and *lower* plots show the finger forces and moment of force of the index (I), middle (M), ring (R), and little (L) fingers. Positive moment direction represents supination efforts.

($p > 0.1$). At DUR-phase when the task-performance variable changed, both components were larger: ME ($p < 0.05$) and nME ($p < 0.001$). These results were observed for both F_{TOT} and M_{TOT} performance variables. The direction of target jump had an effect in the F_{TOT} analysis: the amount of ME ($p < 0.001$) was larger in F+ compared to F− target jumps (see DUR- in the upper-left plots, Fig. 5). Finally, when the target returned to the initial position in the POST-phase, both ME and nME components were larger as compared to the PRE-phase, the time interval before the target jumps, but the relative increase in the ME component was larger. These findings across subjects are illustrated with the group means presented in Fig. 5.

In contrast, for the frozen-feedback variable (lower plots of Fig. 5) the ANOVA revealed a significant interaction *Projection Component* × *Phase* ($F_{1.870,13.083} = 12.310$; $p < 0.05$) for F_{TOT} and a significant interaction *Projection Component* × *Phase* × *Direction* ($F_{1.258,8.807} = 7.081$; $p < 0.05$) for M_{TOT}. Both ME and nME components increased at phases DUR- and POST-leading to no difference between the two in the final state ($p > 0.9$). For the M_{TOT} analysis, the increase in the ME ($p < 0.05$) and nME ($p < 0.0001$) components was larger in the Jumping-Variable F+ than F− (see these differences in the DUR-phase, lower left plot of Fig. 5).

Analysis of the structure of variance. Analysis of the inter-trial variance in the space of finger modes is illustrated in Fig. 6 with the group means for the two variance components (V_{UCM} – gray; V_{ORT} – black). The upper plots show the data for the continuous-feedback variable. For F_{TOT}, the inequality $V_{UCM} > V_{ORT}$ was evident across the three phases while the M_{TOT} differences in V_{UCM} and V_{ORT} approached significance ($F_{1,7} = 4.855$; $p = 0.063$). F_{TOT} showed larger V_{UCM} for F+ Jumping-Variable than when the target jumped to lower levels of force production in F−. The lower plots (Fig. 6) illustrate the data for the frozen-feedback

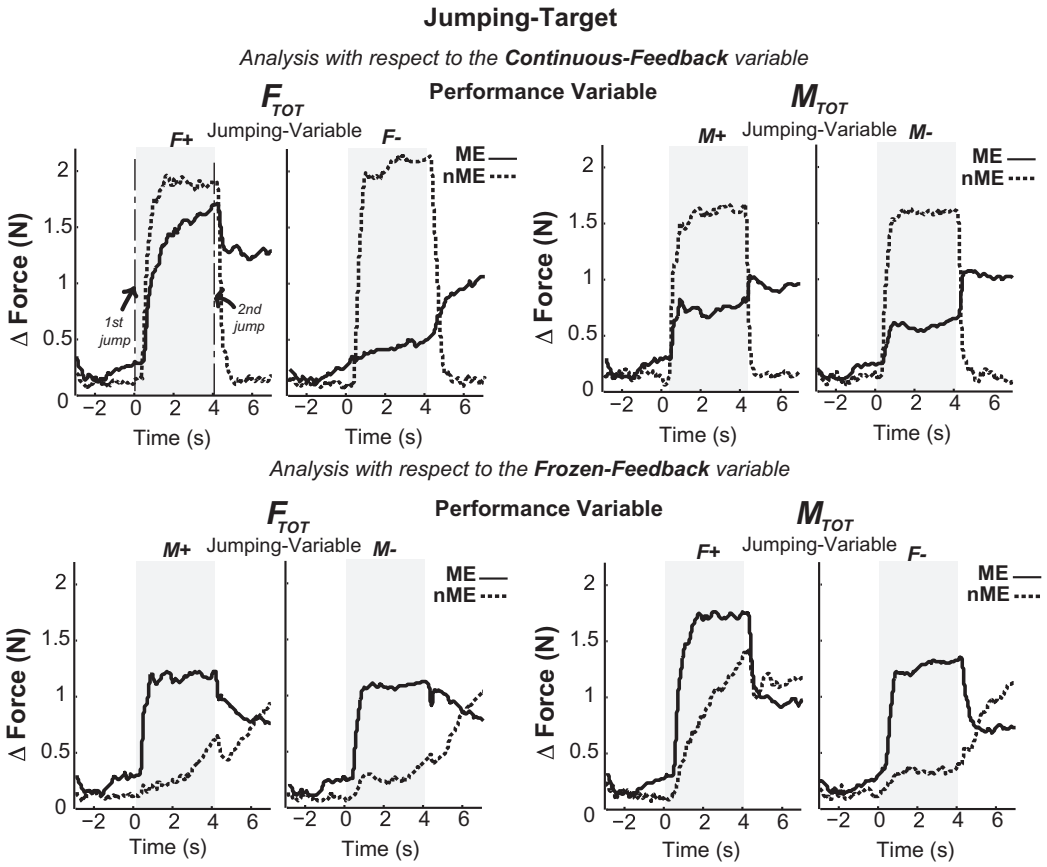

Fig. 4. Typical time profiles of the motor equivalence (ME, solid line) and non-motor equivalence (nME, dotted line) components during the Jumping-Target task. An analysis was performed in the space of finger-modes. Each component was normalized by the square root of the number of DOF in each dimension.

variable. When visual feedback was removed following the first jump, the V_{UCM} and V_{ORT} components became similar (all $p > 0.2$). The 3-way ANOVA revealed a significant effect of *Projection Component* ($F_{1,7} = 5.650$; $p < 0.05$) for F_{TOT}. In contrast, for M_{TOT} analysis, there was only a significant interaction *Projection Component* × *Phase* × *Direction* ($F_{1.372,9.602} = 5.553$; $p < 0.05$). In the analysis with respect to M_{TOT}, V_{ORT} was larger in the F+ jumps than in the F− at DUR- ($p < 0.05$) and POST- ($p < 0.05$) phases. The difference in the amount of V_{UCM} in F+ versus F− during the target jump (DUR-) was close to significance ($p = 0.060$). These results were supported by a significant *Phase* × *Direction* ($F_{1.604,11.229} = 25.573$; $p < 0.0001$) and *Projection Component* × *Direction* ($F_{1.903,13.322} = 4.855$; $p < 0.001$) interactions in the M_{TOT}-analysis.

I-Perturbation tasks

The step perturbation of the I-finger led to different adjustments in the finger forces and modes depending on the visual feedback provided. Fig. 7 illustrates typical time profiles of F_{TOT} and M_{TOT} (top panels) and of the individual finger forces and moments for the continuous and frozen-feedback variables (middle and bottom panels) for a representative subject. The left plots show the time series for the F-task, when F_{TOT} was the continuous-feedback variable and M_{TOT} was the frozen-feedback variable. The right plots show the data for the M-task: M_{TOT} was the continuous-feedback variable and F_{TOT} was the frozen-feedback variable. The time window highlighted in gray corresponds to the lifting of the I-finger by 1 cm.

Note that the values of the continuous-feedback variable (F_{TOT} for F-task, and M_{TOT} for the M-task) were similar PRE- and POST-perturbation. The group average ± SE of F_{TOT} was 11.08 ± 3.27 N and 11.08 ± 3.15 N ($t_7 = 0.08$, $p > 0.90$) PRE- and POST-perturbation, respectively; the average values of M_{TOT} were 0.19 ± 0.42 Nm and 0.01 ± 0.48 Nm, respectively ($t_7 = 0.0843$, $p > 0.42$). In contrast, the frozen-feedback variable showed major deviation from its initial values. In particular, M_{TOT} in the F-task drifted toward negative values (pronation), from −0.08 ± 0.65 Nm to −13.05 ± 7.35 Nm ($t_7 = 5.260$, $p < 0.001$). In the M-task, the changes in F_{TOT} after the visual feedback removal were inconsistent across subjects, the mean values PRE- and POST-perturbation were 11.02 ± 3.20 N and 9.41 ± 4.63 N ($t_7 = 1.044$, $p > 0.33$).

In the F-task, after the I-finger was lifted, the force of the I-finger increased ($t_7 = -4.623$, $p < 0.01$) while the M, R and L fingers showed a force drop ($t_7 > 2.581$, $p < 0.05$). The individual finger moments also changed.

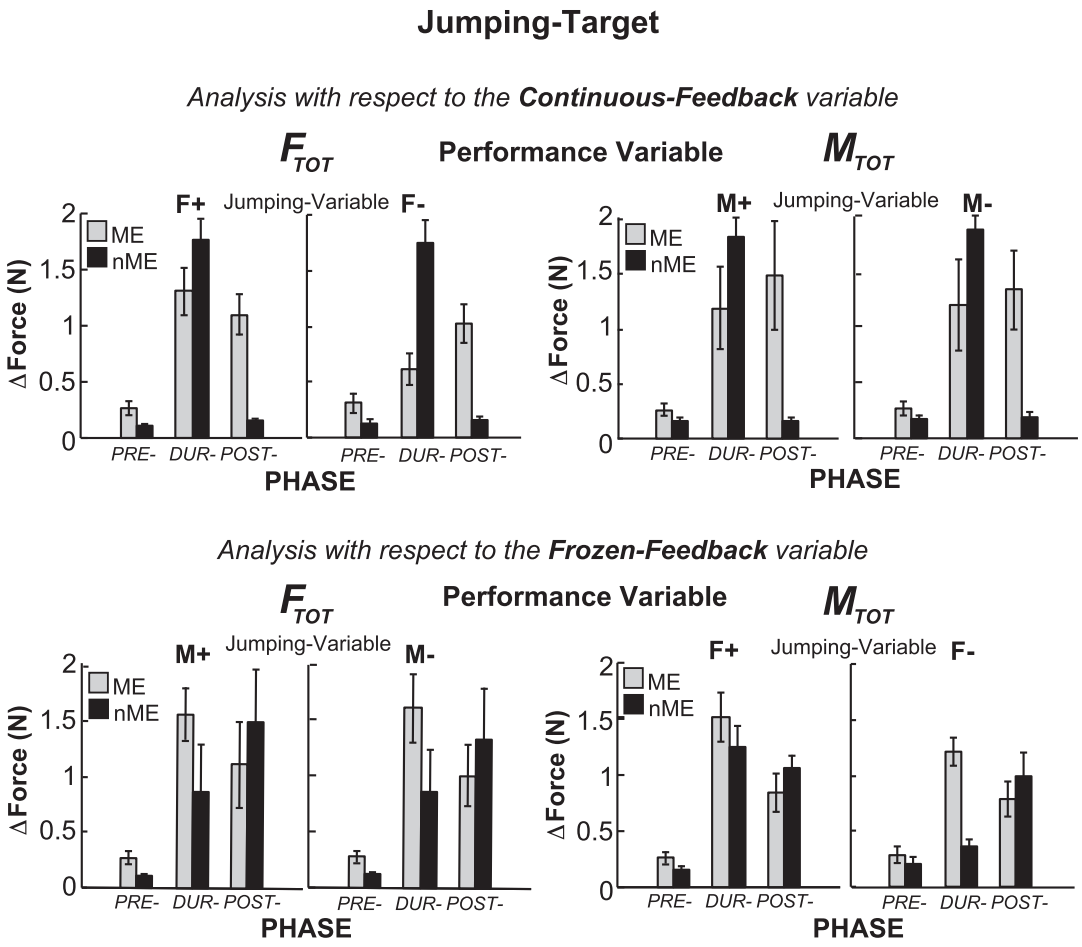

Fig. 5. Group means (±SE) of the motor equivalence (ME, gray bars) and non-motor equivalence (nME, black bars) components at phases: PRE-, during (DUR-), and POST-target-jump. *Upper* and *lower* plots show the continuous-feedback and frozen feedback variables, respectively. Visual feedback was removed for frozen-feedback variables at phases DUR- and POST-Target Jump.

There was an increase in the pronation moment by the I, R and L-fingers ($t_7 > -2.672$, $p < 0.05$). The M-finger was the only one showing a significant increase in the supination moment ($t_7 = -2.581$, $p < 0.05$) post-perturbation.

In the M-task, when the I-finger was lifted, the changes observed for the individual finger forces and moments varied across subjects. The differences between the individual finger forces produced PRE- and POST-perturbation were not significant (all $t_7 < 1.84$, $p > 0.10$). Also, no statistical significance was found in the moment of force of individual fingers between the conditions PRE- and POST-perturbation (all $t_7 < -1.84$, $p > 0.10$).

Motor equivalence analysis. The time profiles of the ME and nME components for a representative subject are illustrated in Fig. 8. For the continuous-feedback variable (top panels), there was an increase in the ME component (solid line) accompanied by minor changes in the nME component (dotted line) from the initial steady state to the final steady state (after the gray area). In contrast, for the frozen-feedback variable (bottom panels), the ME component increased after the I-finger perturbation, but the increase of the nME component was also large. The respective group averages from the motor equivalence analysis are illustrated in Fig. 9. Note the different scales of the *y*-axes in the top (PRE-perturbation) and bottom (POST-perturbation) panels.

Prior to the perturbation, the ME component was larger than the nME component across tasks for the F_{TOT} performance variable ($F_{1,7} = 16.415$; $p < 0.01$), and this difference was close to significance for M_{TOT} ($F_{1,7} = 4.622$; $p = 0.068$). Because the motor equivalence analysis within the phase prior to the perturbation computes a difference vector that is mean free, the ME and nME components in this phase are non-zero because the lengths of difference vectors are positive numbers. The larger ME relative to the nME component may come from the larger variance within the UCM than within ORT, a contamination of the mean by variance for positive measures (see Discussion). In the post-perturbation phase, the difference between ME and nME components was significant both for F_{TOT} ($p < 0.01$) and M_{TOT} ($p < 0.05$) continuous-feedback variables. There was no difference between these components for the frozen-feedback variable, this was true for both performance variables (all $p > 0.1$).

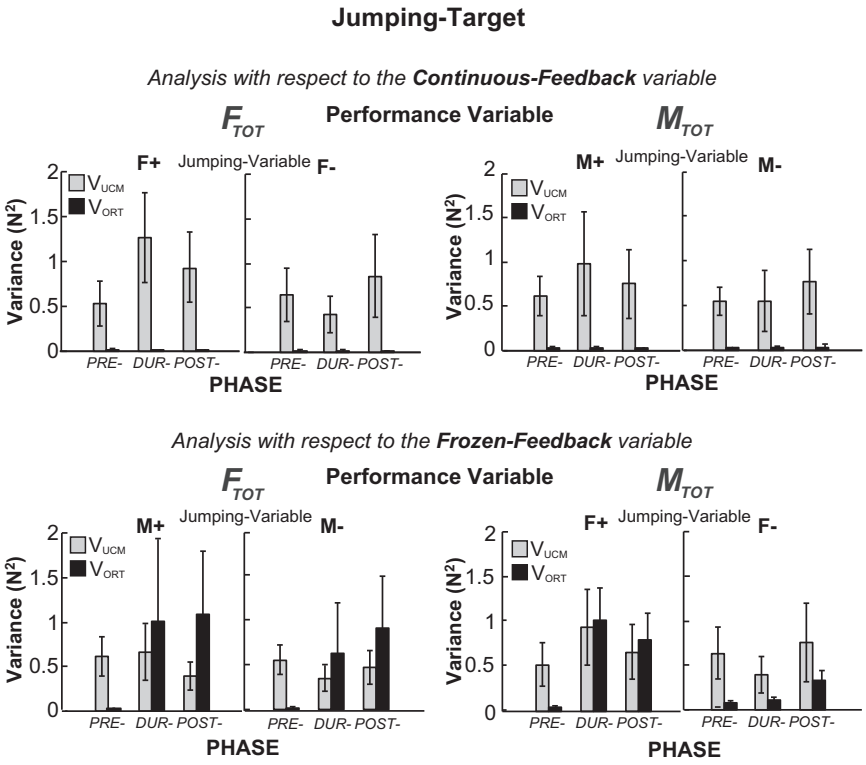

Fig. 6. Group mean (±SE) of the V_{UCM} (gray bars) and V_{ORT} (black bars) components at phases: PRE-, during (DUR-), and POST-target-jump. The continuous-feedback and frozen feedback variables are shown in the *upper* and *lower* plots, respectively.

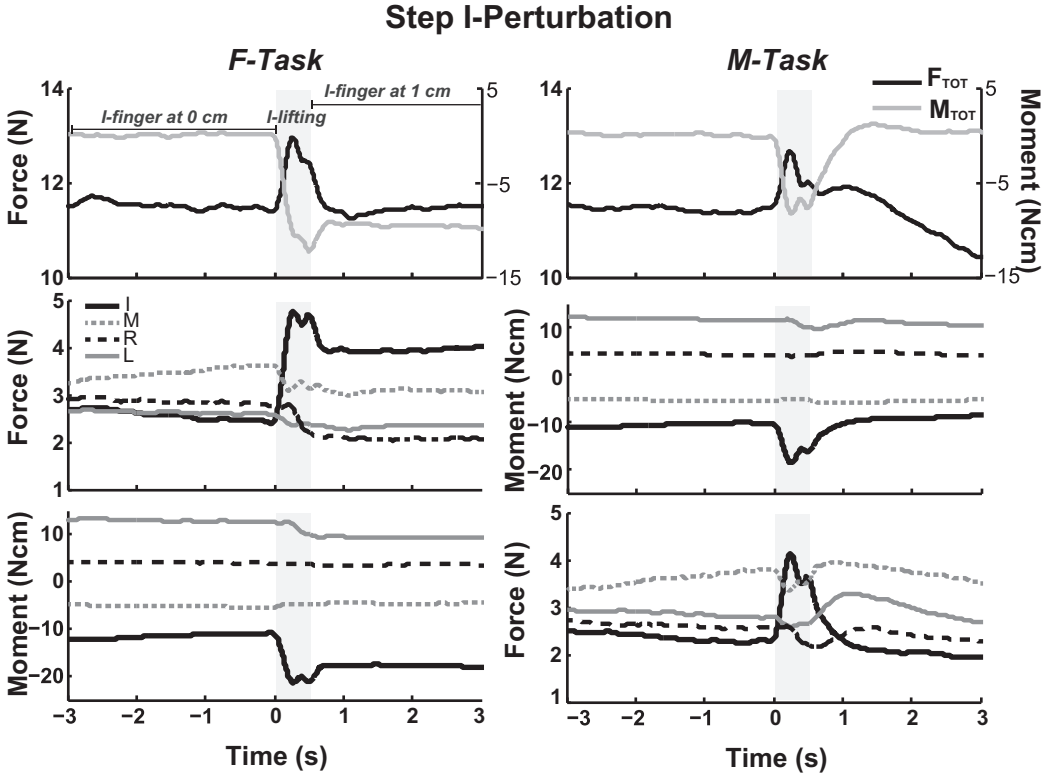

Fig. 7. Force and moment time profiles of a subject during the Step I-Perturbation task. The period highlighted in gray shows the period of lifting of the index (I)-finger. *Upper* plots show the total force (F_{TOT}) and the total moment of force (M_{TOT}) for the F-task and M-task. *Middle* and *lower* plots show the finger forces and moment of force of the index (I), middle (M), ring (R), and little (L) fingers.

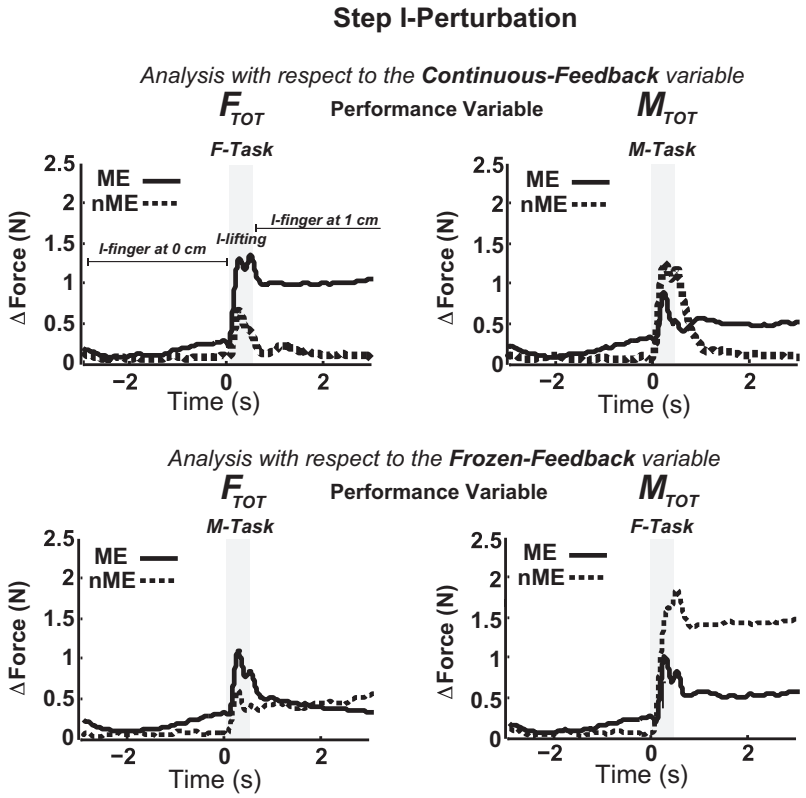

Fig. 8. Typical time profiles of the motor equivalence (ME, solid line) and non-motor equivalence (nME, dotted line) components during the Step I-Perturbation task. Analysis was performed in the space of finger-modes. Each component was normalized by the square root of the number of DOF in each dimension.

Regarding the effects of the perturbation, there was an increase in the ME component at the post-perturbed phase for both tasks. In the F_{TOT}-analysis, the increase in ME was smaller for the frozen- as compared to the continuous-feedback variable (Sig. *Phase* × *Task*: $F_{1,7} = 8.603$; $p < 0.05$), while the ME increase was similar in both tasks with respect to M_{TOT} despite the differences in feedback (Sig. *Phase*: $F_{1,7} = 12.284$; $p < 0.01$). When continuous feedback was provided to the subjects there was no difference in the nME component between the PRE- and POST-conditions (the top and bottom panels have different y-scales) indicating that values of the task-performance were preserved. However, this was not true when visual feedback was removed. In this case, there was a larger nME in F_{TOT} (right panel, Sig. *Phase* × *Task*: $F_{1,7} = 6.255$; $p < 0.05$) and M_{TOT} (left panel, Sig. *Phase* × *Task*: $F_{1,7} = 26.102$; $p = 0.001$) analyses. These findings were supported by a significant interaction *Projection Component* × *Phase* × *Task* computed separately for each task performance variable F_{TOT} ($F_{1,7} = 10.050$; $p < 0.05$) and M_{TOT} ($F_{1,7} = 21.268$; $p < 0.005$).

Analysis of the structure of variance. We performed the variance analysis to verify whether the structure of variance would preserve salient performance variables prior to and after the perturbation of the index finger, and to explore the effects of the visual feedback removal. The group average results of this analysis prior to and after the I-perturbation are illustrated in Fig. 10 in the upper and lower plots, respectively. At the PRE-perturbation phase, feedback was provided for both F_{TOT} and M_{TOT}. Therefore, no differences were expected in the structure of variance prior to the perturbation.

The across-trial variance in finger-mode was structured ($V_{UCM} > V_{ORT}$) to preserve F_{TOT} at both phases when continuous feedback was provided (*Projection Component:* $F_{1,7} = 7.023$; $p < 0.05$). Similar finger-mode structure ($V_{UCM} > V_{ORT}$) was observed for the M-task at pre-perturbation ($t_7 = 3.189$; $p < 0.05$). The visual feedback removal led to a significant increase in V_{ORT} ($t_7 = -3.127$; $p < 0.05$) and no difference in V_{UCM} ($t_7 = -0.946$; $p = 0.376$); as a result, post-perturbation $V_{UCM} \sim V_{ORT}$ ($t_7 = -0.132$; $p = 0.899$). This finding was supported by a significant *Projection Component* × *Phase* interaction ($F_{1,7} = 6.293$; $p < 0.05$). In the M_{TOT} analysis, $V_{UCM} > V_{ORT}$ for the continuous-feedback variable ($F_{1,7} = 8.790$; $p < 0.05$), and for the frozen-feedback variable this difference approached significance ($F_{1,7} = 4.430$; $p = 0.073$) without other effects.

DISCUSSION

The results largely support the main hypothesis that the ME and nME components during quick actions and corrections are task-specific. In particular, we found a larger increase in the ME component when the task a

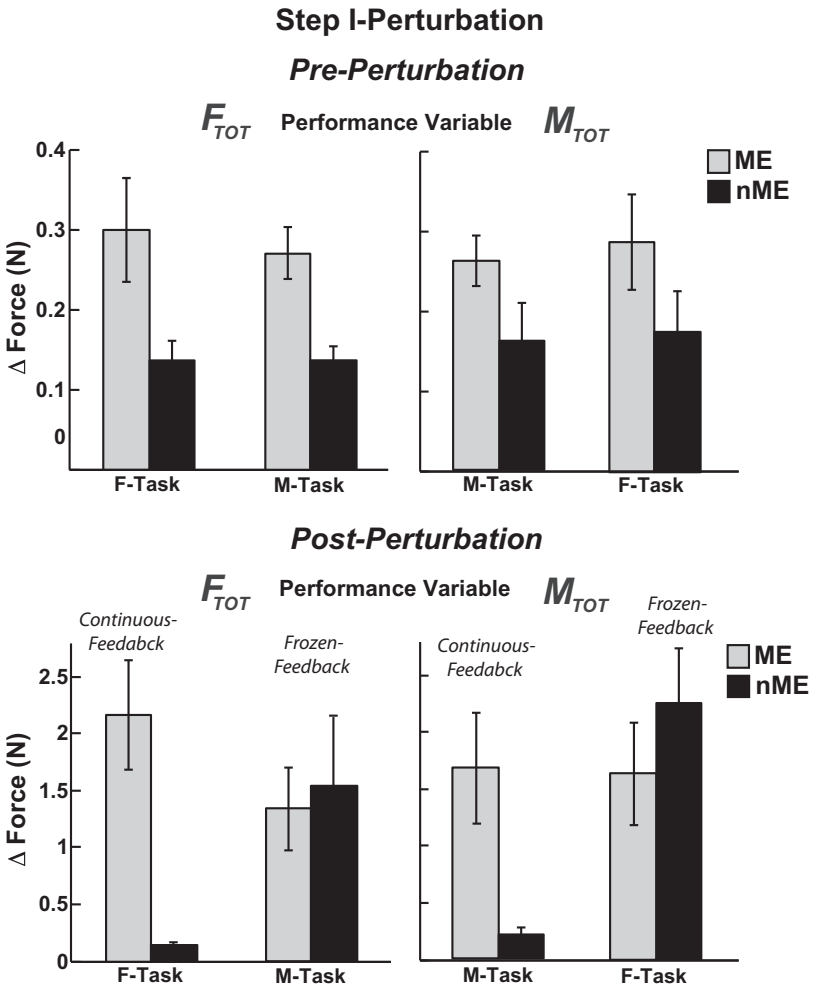

Fig. 9. Group mean (±SE) of the motor equivalence (ME, gray bars) and non-motor equivalence (nME, back bars) components during the Step I-Perturbation task at phases Pre-Perturbation (*upper*-plot) and Post-Perturbation (*lower*-plot). The scale of the *y*-axis is not consistent between plots.

priori required a change only in the nME component during the target jump for each of the two performance variables, but only when this variable was the instructed one. More importantly, after the sequence of target jumps, the nME component returned to values close to pre-perturbed ones with the overall close to zero motion, while the ME motion remained large. A larger ME effect (ME > nME) was also found after the step perturbations of the index finger. The effects of visual feedback removal were mostly along the ORT component resulting in a dramatic increase in the nME component. Further, we discuss implications of these findings on issues of the neural control of redundant (abundant) systems and task-specific stability of performance.

Task-specific stability in abundant systems

Traditional methods to study stability involve the application of small perturbations to the system of interest. Within the UCM hypothesis, an analysis of inter-trial variance has been used to produce indices reflecting stability of multi-element systems in different directions. Assuming somewhat different initial conditions and force fields across trials, one expects relatively high inter-trial variance in less stable directions and low inter-trial variance in more stable directions. Relatively recently a complementary method has been introduced based on observation of system's trajectories during quick actions (Mattos et al., 2011; Scholz et al., 2011). This method assumes that a neural input into the system associated with a quick action may be viewed as a perturbation expected to cause relatively large deviations of the system in directions of low-stability. If a system produces a desired value or time profile of a salient performance variable, large deviations in directions that keep this variable unchanged ME are expected. Large ME deviations have been observed in several earlier studies (Scholz et al., 2007, 2011; Mattos et al., 2011, 2013, 2015).

In all of the mentioned studies, mechanical perturbations were applied and the system's response was quantified. Our study is the first to document large ME deviations during quick actions of a multi-element system in the absence of any perturbations. Indeed, in the jumping-target trials, ME was quantified after a sequence of target jumps on the computer screen leading to the same final combination of F_{TOT} and M_{TOT}. The preservation of the ME > nME after the target

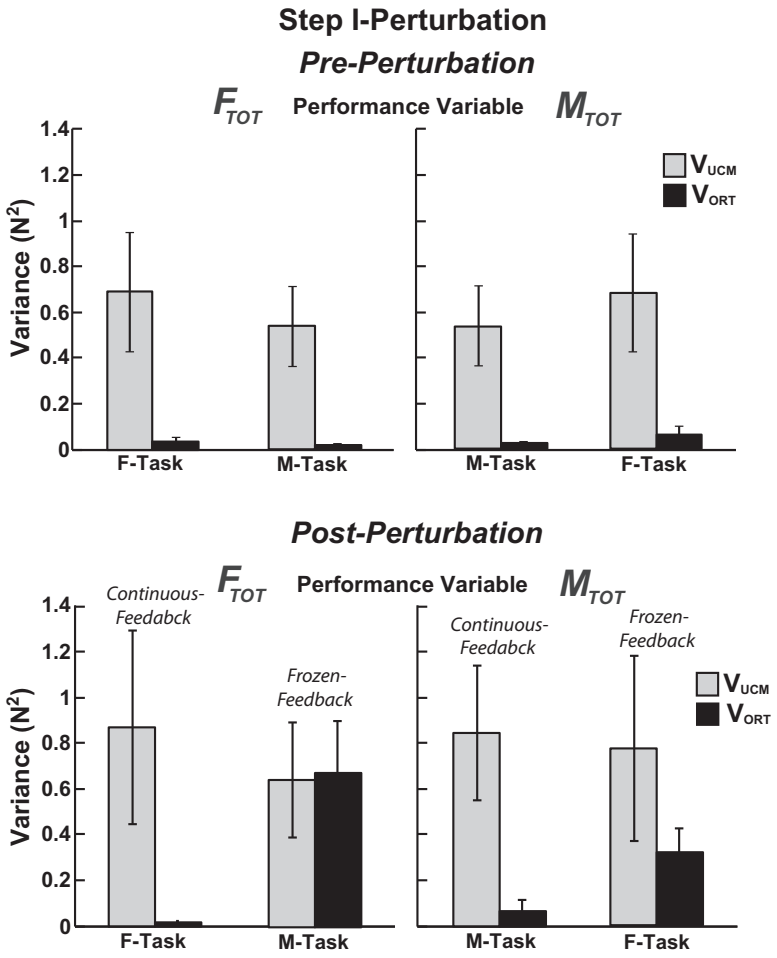

Fig. 10. Group mean (±SE) of the V_{UCM} (gray bars) and V_{ORT} (back bars) components during the Step I-Perturbation task at phases Pre-Perturbation (*upper*-plot) and Post-Perturbation (*lower*-plot).

jumps was task-specific, i.e. F_{TOT} stabilization was observed for the F-task; similarly, M_{TOT} was stabilized during the M-task as reflected by ME > nME. The second condition resembled previous experiments in using perturbations to the elements (cf. Mattos et al., 2011, 2013, 2015). While only one finger was explicitly perturbed (the index finger), all finger forces were affected partly due to the well-known phenomenon of enslaving (lack of individualization, Schieber, 1991; Kilbreath and Gandevia, 1994; Zatsiorsky et al., 1998) and partly due to the mechanical coupling among the fingers. Both conditions showed large ME deviations while nME deviations could differ depending on the available feedback.

We illustrate the idea of task-specific stability and the two methods of its analysis (inter-trial variance and ME) in Fig. 11. Imagine that a person presses with two fingers to produce a certain level of force ($F_1 + F_2 = 10$ N) several times. The cloud of data points across repetitive trials may form an ellipsoid with the major axis parallel to the solution subspace (the UCM, the slanted solid line). Such data distributions are characterized by the inequality $V_{UCM} > V_{ORT}$ and have been interpreted as signatures of a two-finger force-stabilizing synergy (Latash et al., 2001; Scholz et al., 2002). They reflect lower stability of the two-finger system along the UCM as compared to the orthogonal (ORT) direction.

Now, consider that a perturbation is introduced into the system, for example one of the fingers is lifted. This would lead to a change in the force produced by both fingers. There will be an error in the task performance ($F_1 + F_2 > 10$ N). Note, however, that the system is likely to deviate along both ORT and UCM directions, and the deviation along the UCM direction is ME. If the subject of this mental experiment introduces a correction, total force is expected to drop close to the initial level but the individual finger forces may be expected to deviate along the UCM. These ME deviations have no effect on performance and, therefore, are not corrected. Similar effects may be expected from a voluntary quick total force change to a new level and its return to the initial level (same illustration as in Fig. 11 applies). Such a transient action is expected to lead to ME > nME as it was observed in our experiment.

Structure of variance and motor equivalence

The use of a quantitative analysis of ME within the UCM hypothesis is relatively recent. These studies typically

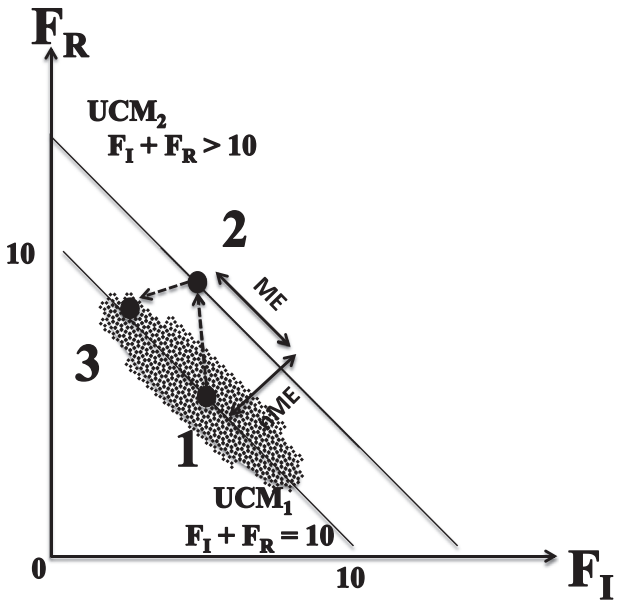

Fig. 11. Scheme illustrating a hypothetical experiment where the goal of the task is to produce 10 N using the index (I) and ring (R)-fingers. When this task is repeated several times, and the force sharing between the I and R fingers (*I,R-sharing*) for each trial is plotted, the shape of the distribution will be an ellipse. The major axis corresponds to all the combinations of finger forces that satisfy the task, i.e. the UCM. Now, lets assume that one of the fingers is perturbed (eg. lifting of the I-finger) leading to increase in the force produced by both fingers. The total force will be larger than 10 N. Then, after some delay, the force of the I and R-fingers will decrease to maintain the total force close to 10 N, representing motor equivalence at the task-performance. It is likely that the force produced by the individual fingers will change relative to the unperturbed state. The *I, R-sharing* is illustrated in three states: 1-unperturbed, 2-during the perturbation; 3-after the correction. Note that most of the deviations in *I, R-sharing* lie along the UCM (ME component) as compared with deviations orthogonal to the UCM (nME component).

measured ME after either external perturbations applied to the whole system (Scholz et al., 2007), or to some of its elements (Mattos et al., 2011, 2013, 2015), or as a consequence of modified movement dynamics due to changes in the speed of reaching by a multi-joint effector (Scholz et al., 2011). The common finding among these studies is that ME deviations become larger with time after the perturbation and get contributions from mechanical reactions, reflex responses, and also voluntary corrections.

In this study we used two methods to quantify stability in a multi-elemental system. Both methods are indirect: They produce indices that may be used as proxies of dynamic stability. An analysis of the structure of inter-trial variance produces indices reflecting deviations of trajectories from an assumed desired one in two subspaces. This method is based on an assumption that the subject is trying "to do the same" across repetitive trials, and variance indices reflect the natural behavior of the involved systems. An analysis of motor equivalence assumes that neural circuits involved in task-specific stability respond similarly to inputs from both periphery (such as those induced by perturbations) and hierarchically higher neural level (such as those induced by quick actions).

According to the general scheme (as in Fig. 11), both ME and structure of variance reflect task-specific stability. They, however, show different sensitivity to aspects of the action. For example, the system may show large deviations in a performance variable from an initial state resulting in large nME component such that ME < nME (Figs. 4 and 5). It may still be characterized by the $V_{UCM} > V_{ORT}$ inequality in both the initial and the final states (Fig. 6). On the other hand, V_{UCM} shows high sensitivity to the magnitude of the performance variable (V_{UCM}) while V_{ORT} shows high sensitivity to its rate (Goodman et al., 2005; Friedman et al., 2011), thus it is possible to observe $V_{ORT} > V_{UCM}$ (or $V_{ORT} \sim V_{UCM}$) accompanied by ME > nME (Mattos et al., 2015).

The ME effect (ME > nME) and the variance structure can also influence one another. Such interaction is expected when the difference of a finger-mode vector (Δm_j) from the pre-perturbed average is small, for example in the PRE-phase of the Jumping-Target and Step I-Perturbation tasks. The ME/nME components are computed as the length of the projections of the Δm_j, i.e. positive numbers. The mean Δm_j is zero in the PRE-phase. However, both ME and nME components are positive and their means are non-zero. For a broader data distribution, such an operation results in the mean shifted to larger values (Hansen et al., 2015). Because the variance of the data is larger in the UCM than in ORT, ME > nME is expected for small deviations from the mean. However, this type of interaction does not dominate in the POST-phase when Δm_j values are certainly different from zero.

An additional observation was that the difference in the structure of the inter-trial variance was different for different force levels required during the target jumps. When the target jumped to forces corresponding to 20% of the MVC there was a strong force-stabilizing synergy in a sense $V_{UCM} > V_{ORT}$. However, the target jumps to lower levels of force (10% of the MVC) resulted in $V_{ORT} \sim V_{UCM}$. These observations may be related to the mentioned dependence of V_{UCM} on the total force level. While higher force levels lead to more variance (Newell et al., 1984), when an abundant set of fingers is involved in the task, most of the variance is V_{UCM} (Goodman et al., 2005). Also, lower force levels required relaxation of the force producing muscles, which has been shown to lead to more variable performance than that during force increase (Shim et al., 2003, 2005; Li, 2013).

Links to control with referent configurations (RCs)

The ideas of the UCM hypothesis and of the neural control using referent spatial coordinates for salient variables have recently been united into a single scheme (Latash, 2010). The referent configuration (RC) hypothesis 2009 (Feldman, 2009) is a generalization of the equilibrium point-hypothesis (Feldman, 1966, 1986) to multi-effector systems. According to this hypothesis, the CNS specifies a RC of the body, defined as a set of referent coordinates (thresholds of the tonic stretch reflex) at which all the muscles are at their thresholds for

activation. The RC is typically not achievable due to anatomical and external constraints. As a result, the body reaches a state characterized with a non-zero level of muscle activations and non-zero forces on the environment. At the highest, task-specific level, the RC_{TASK} corresponds to referent coordinates for task-specific variables. In particular, in our experiment, setting values of F_{TOT} and M_{TOT} may be associated with setting a vertical referent coordinate for the virtual finger (an imagined digit with the action equivalent to that of all four fingers, Arbib et al., 1985) and an angular referent coordinate (Latash, 2010). These can be observed experimentally, when external forces are removed and the subject does not react to the resulting change in the finger positions (Latash et al., 2010). Since conditions in our study were isometric, the differences between the actual and referent coordinates resulted in the production of non-zero F_{TOT} and M_{TOT}.

The two task-specific referent coordinates result in referent coordinates for the four individual fingers; this is an example of a redundant problem (Bernstein, 1967). In our analysis we assume that the four finger-level referent coordinates are reflected in the four finger modes. If only one mode referent coordinate is involved, removing the stop and allowing the fingers to move is expected to result in a combination of displacements of all four fingers. We assume that this two-to-four transformation is organized in a synergic way, which means that any spontaneous deviations in individual finger referent coordinates happen primarily in a sub-space that does not affect the performance variables (the UCM). This leads to the characteristic inequality $V_{UCM} > V_{ORT}$. Within this study, we do not address the next levels within the motor control hierarchy, which are also organized in a similar way, for example the transformation from finger referent coordinates to referent coordinates for the many muscles affecting each finger's action.

Any intentional action is expected to be organized at the highest level of the hierarchy and represent shifts of referent coordinates for F_{TOT} and M_{TOT}. By itself, the action does not specify actions of individual fingers and referent coordinates for fingers change according to the mentioned task-specific synergic organization. This ensures stability of the F_{TOT} and M_{TOT} pair of variables and is expected to lead to large ME components of finger force (mode) changes and $V_{UCM} > V_{ORT}$. Note that both synergic signatures were observed across tasks and conditions in our study.

Unintentional drift in variables without visual feedback

When visual feedback was provided on one of the two performance variables, the other variable (the frozen-feedback variable) showed a large-amplitude drift despite the instruction to the subjects to keep both variables at the initial levels. Removing visual feedback during steady-state accurate force production tasks is known to lead to a slow drift in the force level (Slifkin et al., 2000; Vaillancourt et al., 2001; Vaillancourt and Russell, 2002; Ambike et al., 2013). In those earlier studies, the subjects were not explicitly instructed to correct target forces, while our subjects were always instructed to keep the F_{TOT} and M_{TOT} values at the target level. A study comparing the two instructions reported more consistent behavior under the "do not interfere" instruction compared to the "correct quickly" instruction (Latash, 1994). Therefore, the instruction used in our experiment to correct the continuous-feedback variable could also play a role in the observed inconsistent force drifts among subjects.

The drift in M_{TOT} during the changes in force was consistently toward pronation in I-Perturbation trials. In earlier studies, an interpretation has been offered of the force drift (and also of the hand position drift in multi-joint tasks, Zhou et al., 2014, 2015) based on the idea of RC control (Ambike et al., 2013, 2015; Zhou et al., 2014). According to this idea, RC for a performance variable drifts slowly toward the actual value of this variable (RC-back-coupling) reflecting the natural tendency of physical systems to move toward a minimum of potential energy. Note that M_{TOT} was computed with respect to an axis passing through the mid-point between the middle and ring fingers. This was an arbitrarily selected point, which was likely shifted with respect to the point of application of the resultant finger force during natural pressing tasks closer to the middle finger (Scholz et al., 2002). So, it was possible that in the absence of visual feedback the computed M_{TOT} drifted toward a value corresponding to the preferred point of application of the resultant.

CONCLUSION

The main message of this study is that ME is a robust phenomenon that is observed following a sequence of quick actions leading to the same values of task-specific performance variables. Hence, voluntary actions may be viewed as descending perturbations into abundant systems. This finding supports the scheme of motor control based on the idea that a family of solutions is facilitated to stabilize values of important performance variables.

Acknowledgments—The study was supported by NIH grants NS-035032 and AR-048563.

REFERENCES

Ambike S, Paclet F, Latash ML, Zatsiorsky VM (2013) Grip-force modulation in multi-finger prehension during wrist flexion and extension. Exp Brain Res 227:509–522.

Ambike S, Zatsiorsky VM, Latash ML (2015) Processes underlying unintentional finger-force changes in the absence of visual feedback. Exp Brain Res 233:711–721.

Arbib MA, Iberall T, Lyons D (1985) Coordinated control programs for movements on the hand. In: Goodwin AW, Darian-Smith I, editors. Hand function and the neocortex. Berlin: Springer Verlag. p. 111–129.

Bernstein NA (1967) The coordination and regulation of movements. Oxford: Pergamon Press.

Danion F, Schoner G, Latash ML, Li S, Scholz JP, Zatsiorsky VM (2003) A mode hypothesis for finger interaction during multi-finger force-production tasks. Biol Cybern 88:91–98.

Feldman AG (1966) On the functional tuning of the nervous system in movement control or preservation of stationary pose. II. Adjustable parameters in muscles. Biofizika 11:498–508.
Feldman AG (1986) Once more on the equilibrium-point hypothesis (l model) for motor control. J Mot Behav 18:17–54.
Feldman AG (2009) Origin and advances of the equilibrium-point hypothesis. Adv Exp Med Biol 629:637–643.
Friedman J, Latash ML, Zatsiorsky VM (2011) Directional variability of the isometric force vector produced by the human hand in multijoint planar tasks. J Mot Behav 43:451–463.
Gelfand IM, Latash ML (1998) On the problem of adequate language in motor control. Motor Control 2:306–313.
Goodman SR, Shim JK, Zatsiorsky VM, Latash ML (2005) Motor variability within a multi-effector system: experimental and analytical studies of multi-finger production of quick force pulses. Exp Brain Res 163:75–85.
Hansen E, Grimme B, Reimann H, Schoner G (2015) Carry-over coarticulation in joint angles. Exp Brain Res 233:2555–2569.
Kilbreath SL, Gandevia SC (1994) Limited independent flexion of the thumb and fingers in human subjects. J Physiol 479:487–497.
Latash ML (1994) Reconstruction of equilibrium trajectories and joint stiffness patterns during single-joint voluntary movements under different instructions. Biol Cybern 71:441–450.
Latash ML (2010) Motor synergies and the equilibrium-point hypothesis. Motor Control 14:294–322.
Latash ML (2012) The bliss (not the problem) of motor abundance (not redundancy). Exp Brain Res 217:1–5.
Latash ML, Friedman J, Kim SW, Feldman AG, Zatsiorsky VM (2010) Prehension synergies and control with referent hand configurations. Exp Brain Res 202:213–229.
Latash ML, Scholz JF, Danion F, Schoner G (2001) Structure of motor variability in marginally redundant multifinger force production tasks. Exp Brain Res 141:153–165.
Latash ML, Shim JK, Smilga AV, Zatsiorsky VM (2005) A central back-coupling hypothesis on the organization of motor synergies: a physical metaphor and a neural model. Biol Cybern 92:186–191.
Li S (2013) Analysis of increasing and decreasing isometric finger force generation and the possible role of the corticospinal system in this process. Motor Control 17:221–237.
Martin JR, Budgeon MK, Zatsiorsky VM, Latash ML (2011) Stabilization of the total force in multi-finger pressing tasks studied with the 'inverse piano' technique. Hum Mov Sci 30:446–458.
Martin V, Scholz JP, Schoner G (2009) Redundancy, self-motion, and motor control. Neural Comput 21:1371–1414.
Mattos D, Kuhl J, Scholz JP, Latash ML (2013) Motor equivalence (ME) during reaching: is ME observable at the muscle level? Motor Control 17:145–175.
Mattos DJ, Latash ML, Park E, Kuhl J, Scholz JP (2011) Unpredictable elbow joint perturbation during reaching results in multijoint motor equivalence. J Neurophysiol 106:1424–1436.
Mattos D, Schoner G, Zatsiorsky VM, Latash ML (2015) Motor equivalence during multi-finger accurate force production. Exp Brain Res 233:487–502.
Newell KM, Carton LG, Hancock PA (1984) Kinetic analysis of response variability. Psychol Bull 96:133–151.
Pilon J-F, De Serres SJ, Feldman AG (2007) Threshold position control of arm movement with anticipatory increase in grip force. Exp Brain Res 181:49–67.
Prilutsky BI, Zatsiorsky VM (2002) Optimization-based models of muscle coordination. Exerc Sport Sci Rev 30:32–38.
Schieber MH (1991) Individuated finger movements of rhesus monkeys: a means of quantifying the independence of the digits. J Neurophysiol 65:1381–1391.
Scholz JP, Danion F, Latash ML, Schoner G (2002) Understanding finger coordination through analysis of the structure of force variability. Biol Cybern 86:29–39.
Scholz JP, Dwight-Higgin T, Lynch JE, Tseng YW, Martin V, Schoner G (2011) Motor equivalence and self-motion induced by different movement speeds. Exp Brain Res 209:319–332.
Scholz JP, Schoner G (1999) The uncontrolled manifold concept: identifying control variables for a functional task. Exp Brain Res 126:289–306.
Scholz JP, Schoner G, Hsu WL, Jeka JJ, Horak F, Martin V (2007) Motor equivalent control of the center of mass in response to support surface perturbations. Exp Brain Res 180:163–179.
Schoner G (1995) Recent developments and problem in human movement science and their conceptual implications. Ecol Psychol 7:291–314.
Shim JK, Latash ML, Zatsiorsky VM (2003) Prehension synergies: trial-to-trial variability and hierarchical organization of stable performance. Exp Brain Res 152:173–184.
Shim JK, Olafsdottir H, Zatsiorsky VM, Latash ML (2005) The emergence and disappearance of multi-digit synergies during force-production tasks. Exp Brain Res 164:260–270.
Slifkin AB, Vaillancourt DE, Newell KM (2000) Intermittency in the control of continuous force production. J Neurophysiol 84:1708–1718.
Turvey MT (1990) Coordination. Am Psychol 45:938–953.
Vaillancourt DE, Russell DM (2002) Temporal capacity of short-term visuomotor memory in continuous force production. Exp Brain Res 145:275–285.
Vaillancourt DE, Slifkin AB, Newell KM (2001) Intermittency in the visual control of force in Parkinson's disease. Exp Brain Res 138:118–127.
Vereijken B, Vanemmerik REA, Whiting HTA, Newell KM (1992) Free (Z)Ing degrees of freedom in skill acquisition. J Mot Behav 24:133–142.
Zatsiorsky VM, Li ZM, Latash ML (1998) Coordinated force production in multi-finger tasks: finger interaction and neural network modeling. Biol Cybern 79:139–150.
Zhou T, Solnik S, Wu YH, Latash ML (2014) Equifinality and its violations in a redundant system: control with referent configurations in a multi-joint positional task. Motor Control 18:405–424.
Zhou T, Zhang L, Latash ML (2015) Characteristics of unintentional movements by a multijoint effector. J Mot Behav 7:1–10.

(Accepted 21 September 2015)
(Available online 3 October 2015)